# Expanded View Figures

**Figure EV1. ZIKV infection of NSCs and induction of autophagy.**

A, B Infection of human NSCs and plaque-forming units for both ZIKV strain (MR766 and Paraiba) at different time points during infection.

C Western blot of autophagy proteins LC3 and P62 at various times after infection of primary mouse NSCs with strains MR766 or Paraiba.

D Densitometric quantification of the blot shown in Fig 1C expressed as the ratio of LC3-II/Gapdh and p62/Gapdh, mean ± SEM of $n = 3$ biological replicates, $^{*}P < 0.05$, $^{**}P < 0.005$, by Student's $t$ test.

E Western blot of LC3-I/LC3-II expression in control or ZIKV-infected NSC treated with or without 100 nM rapamycin, 10 nM bafilomycin A1, or 20 μM chloroquine for 24 h.

F Quantification of the LC3-I/LC3-II ratio from the Western blot shown in (E). Data are presented as the mean ± SEM of two biological replicates. $^{*}P < 0.05$ by Student's $t$ test

G Fluorescence images of GFP-LC3 in NSCs 24 h after mock or ZIKV infection (MR766, MOI 0.2). Cells were incubated with or without 100 nM rapamycin or 5 mM 3-methyladenine. Scale bar = 50 μm.

H Infection of hNSCs and plaque-forming units for ZIKV treated with autophagy activator (rapamycin) and inhibitors (Baf, CQ and 3-MA). Mean ± SEM of three biological triplicates. $^{*}P < 0.05$, $^{**}P < 0.01$, $^{***}P < 0.001$ by Student's $t$ test.

I RT-qPCR showing binding and entry of ZIKV in the presence of rapamycin, baf, CQ, and 3-MA. Mean ± SEM of $n = 3$ biological replicates, ns by Student's $t$ test.

J Western blot analysis showing siRNA-mediated knockdown of autophagy proteins ATG9A, Beclin, and LC3-II.

K Densitometric analysis of KD proteins, mean ± SEM of $n = 3$ biological replicates. $^{*}P < 0.05$ by Student's $t$ test.

L Western blot analysis of LC3-I and LC3-II expression in HeLa cells treated for 4 h with the autophagy inducers perifosine (50 μM), rapamycin (50 nM), and resveratrol (100 μM).

M, N GO analysis of biological processes (M) and cellular localization (N) enriched among the 83 genes commonly downregulated by all three autophagy activators (HeLa cells) and ZIKV infection (hNSCs). Bars represent $-\log_{10} P$ values.

O String analysis of enriched pathways common to both autophagy-induced HeLa cells and ZIKV-infected hNSCs. Edge (line) thickness is proportional to the combined network score, with thicker edges representing stronger evidence for protein interaction.

P RT–qPCR analysis of ZIKV copy number in mNSCs (upper graph) and hNSC (lower graph) at 12, 24, and 36 h post-infection with MR766 (MOI 0.2) and Paraiba (MOI 2) ZIKV. Data are presented as the mean ± SEM of $n = 3$.

Q Mock-infected mNSCs (top row) showing normal morphology of mitochondria, ER, and other cellular organelles. MR766 strain ZIKV-infected mNSCs (middle row) showing many vacuole-like structures, disrupted ER membrane (ER), and localization of viral particles (ZV) to membrane-bound organelles. Paraiba strain ZIKV-infected mNSCs (bottom row) showing many double-membrane-bound autophagosome-like structures and aberrant mitochondria and ER. Scale bars 1 μm (left) and 500 nm (middle and right).

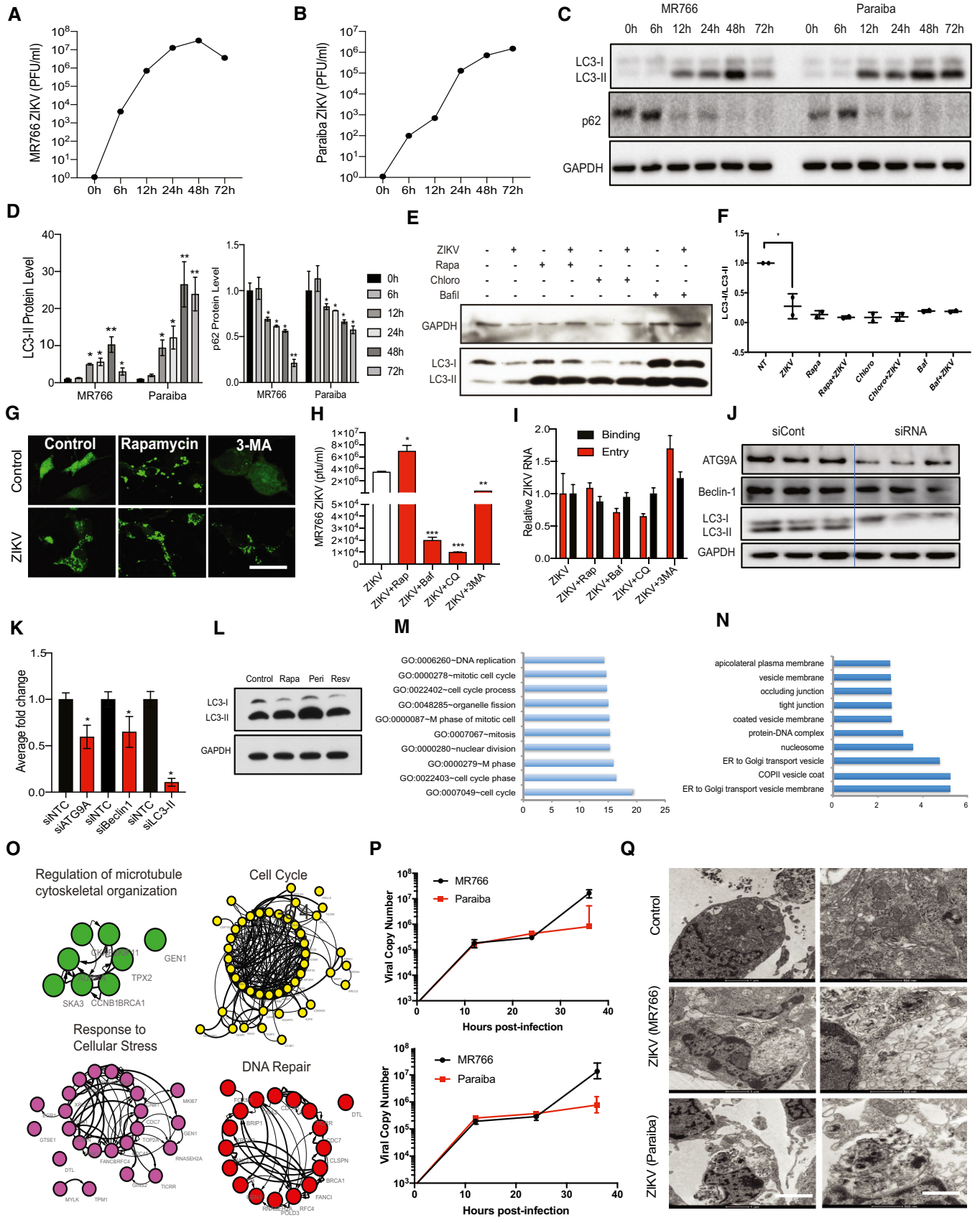
A
MR766 ZIKV (PFU/ml)
0h 6h 12h 24h 48h 72h
B
Paraiba ZIKV (PFU/ml)
0h 6h 12h 24h 48h 72h
C
MR766
Paraiba
0h 6h 12h 24h 48h 72h
LC3-I
LC3-II
p62
GAPDH
D
LC3-II Protein Level
p62 Protein Level
MR766
Paraiba
0h
6h
12h
24h
48h
72h
E
ZIKV
Rapa
Chloro
Bafil
GAPDH
LC3-I
LC3-II
F
LC3-II/LC3-I
NT
ZIKV
Rapa
Rapa+ZIKV
Chloro
Chloro+ZIKV
Baf
Baf+ZIKV
G
Control
Rapamycin
3-MA
Control
ZIKV
H
MR766 ZIKV (pfu/ml)
ZIKV
ZIKV+Rap
ZIKV+Baf
ZIKV+CQ
ZIKV+3MA
I
Binding
Entry
Relative ZIKV RNA
ZIKV
ZIKV+Rap
ZIKV+Baf
ZIKV+CQ
ZIKV+3MA
J
siCont
siRNA
ATG9A
Beclin-1
LC3-I
LC3-II
GAPDH
K
Average fold change
siNTC
siATG9A
siNTC
siBeclin1
siNTC
siLC3-II
L
Control
Rapa
Peri
Resv
LC3-I
LC3-II
GAPDH
M
GO:0006260~DNA replication
GO:0000278~mitotic cell cycle
GO:0022402~cell cycle process
GO:0048285~organelle fission
GO:0000087~M phase of mitotic cell
GO:0007067~mitosis
GO:0000280~nuclear division
GO:0000279~M phase
GO:0022403~cell cycle phase
GO:0007049~cell cycle
N
apicolateral plasma membrane
vesicle membrane
occluding junction
tight junction
coated vesicle membrane
protein-DNA complex
nucleosome
ER to Golgi transport vesicle
COPII vesicle coat
ER to Golgi transport vesicle membrane
O
Regulation of microtubule cytoskeletal organization
Cell Cycle
Response to Cellular Stress
DNA Repair
P
MR766
Paraiba
Viral Copy Number
Hours post-infection
Q
Control
ZIKV (MR766)
ZIKV (Paraiba)

**Figure EV1.**

**Figure EV2. FANCC modulates virophagy in ZIKV-infected cells.**

A Western blot analysis of TOMM20 in ZIKV-infected cells at 12 and 24 h post-infection.

B Western blot analysis of LC3-I, LC3-II, and FANCC expression in mock- or ZIKV-infected HeLa cells expressing a control plasmid or a FANCC overexpression plasmid. Upper panel shows whole cell lysates, and lower panels show subcellular fractions enriched in mitochondria and autophagosomes.

C Confocal immunofluorescence images showing co-labeling of FANCC with LC3-II antibody in hNSC infected with ZIKV (MR766) and control group. Scale bar = 100 μm, boxed magnified images with scale bar = 50 μm.

D, E RT–qPCR analysis of relative expression of FANCC genes in control or ZIKV-infected HeLa cells expressing control plasmid or FANCC overexpression plasmid FANCC (D), or control (NT) or FANCC-specific siRNAs (E). Cells were analyzed at 48 h post-infection. Data are presented as the mean ± SEM of biological triplicates.

F, G RT–qPCR analysis of ZIKV (F) and FANCC (G) gene expression in mock- or ZIKV-infected HeLa cells expressing control (NTC) or FANCC-specific siRNA. Cells were analyzed 24 h post-infection. Data are presented as the mean ± SEM of $n = 3$ biological replicates.

H Immunofluorescence images of ZIKVE expression in ZIKV-infected (MR766, MOI 0.2) HeLa cells after FANCC knockdown (siFANCC) or overexpression (O/E). Cells were stained at 48 h after ZIKV infection. Scale bar = 100 μm.

I, J Relative mRNA expression of FANCC and E2F4 in mNSC, human microglial, macrophage/monocyte (THP-1), and fibroblast (BJ) cell lines at 36 h after ZIKV infection. Mean of biological duplicates.

K Gene ontology analysis of predicted E2F4 target genes downregulated by ZIKV infection. Bars represent $-\log_{10} P$ value.

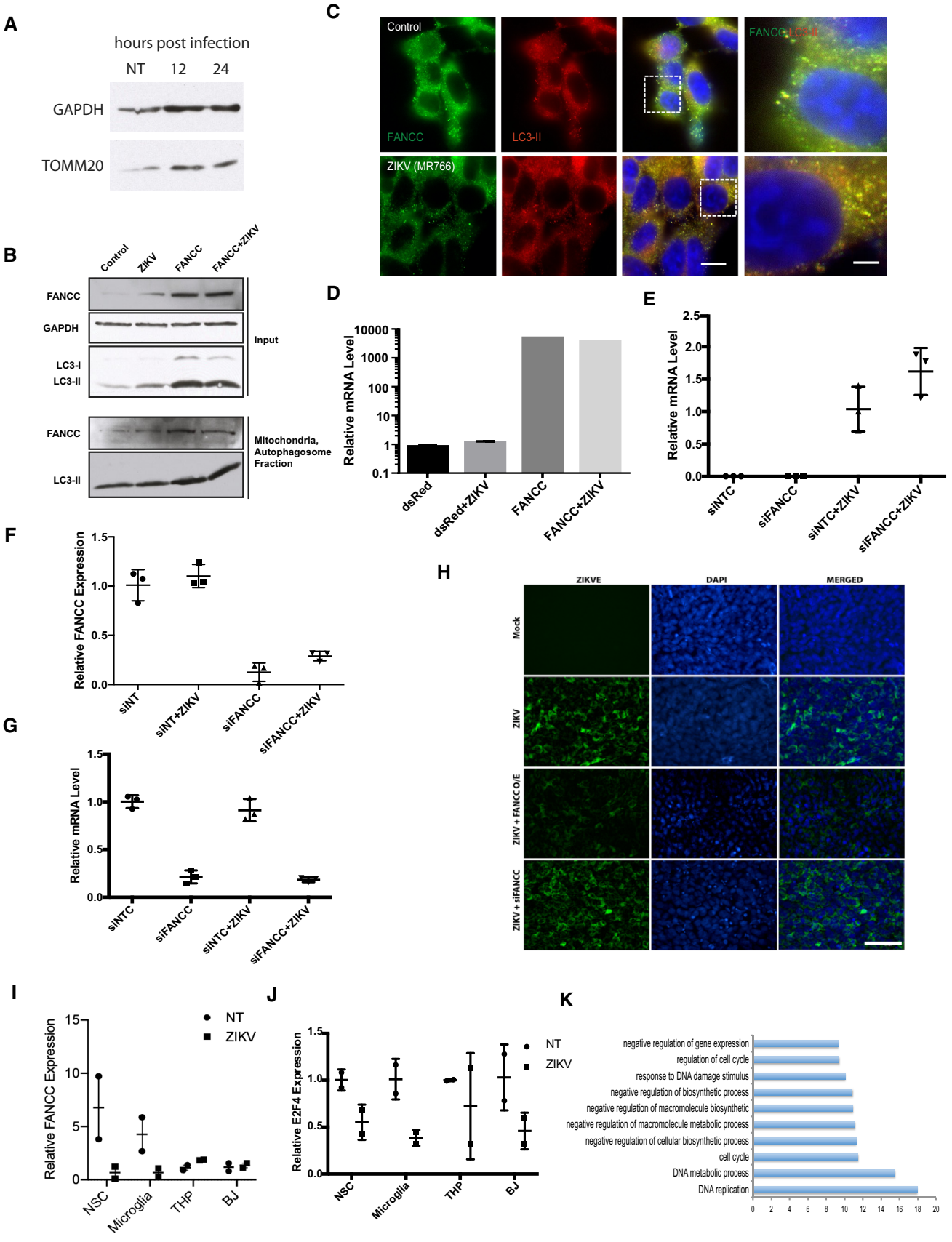


**Figure EV2.**

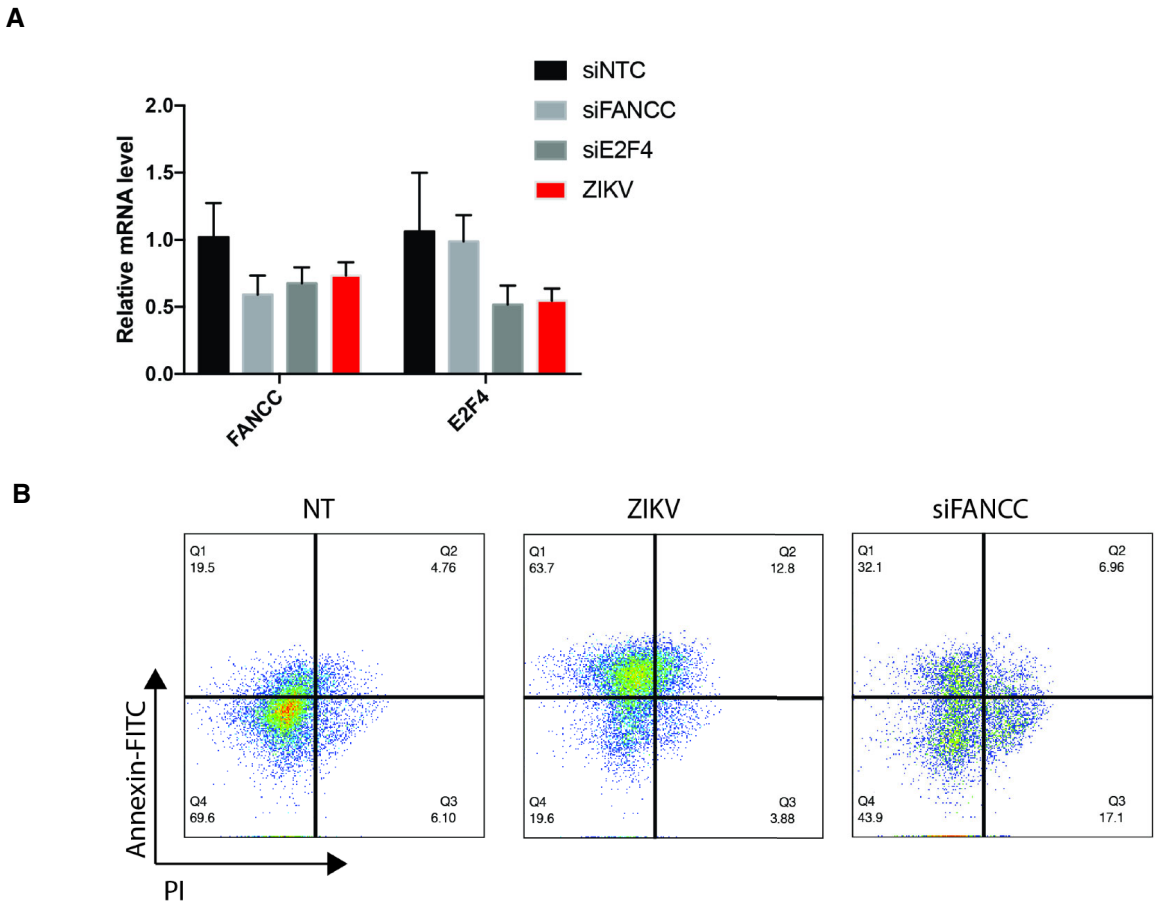


**Figure EV3. ZIKV and FANCC induce autophagy and apoptosis.**

A RT–qPCR analysis of FANCC and E2F4 expression in hNSCs expressing control (NTC), FANCC-specific, or E2F4-specific siRNAs, or infected with ZIKV 48 h post-treatment. Data are presented as the mean ± SEM of biological triplicates.

B Flow cytometric analysis of annexin V and PI staining of hNSCs at 48 h after mock (left), ZIKV infection (middle), or siFANCC transfection (right). Q1, early apoptotic cells (annexin$^+$/PI$^-$); Q2, late apoptotic cells (annexin$^+$/PI$^+$); Q3, necrotic cells (annexin$^-$/PI$^+$); Q4, healthy cells (annexin$^-$/PI$^-$).

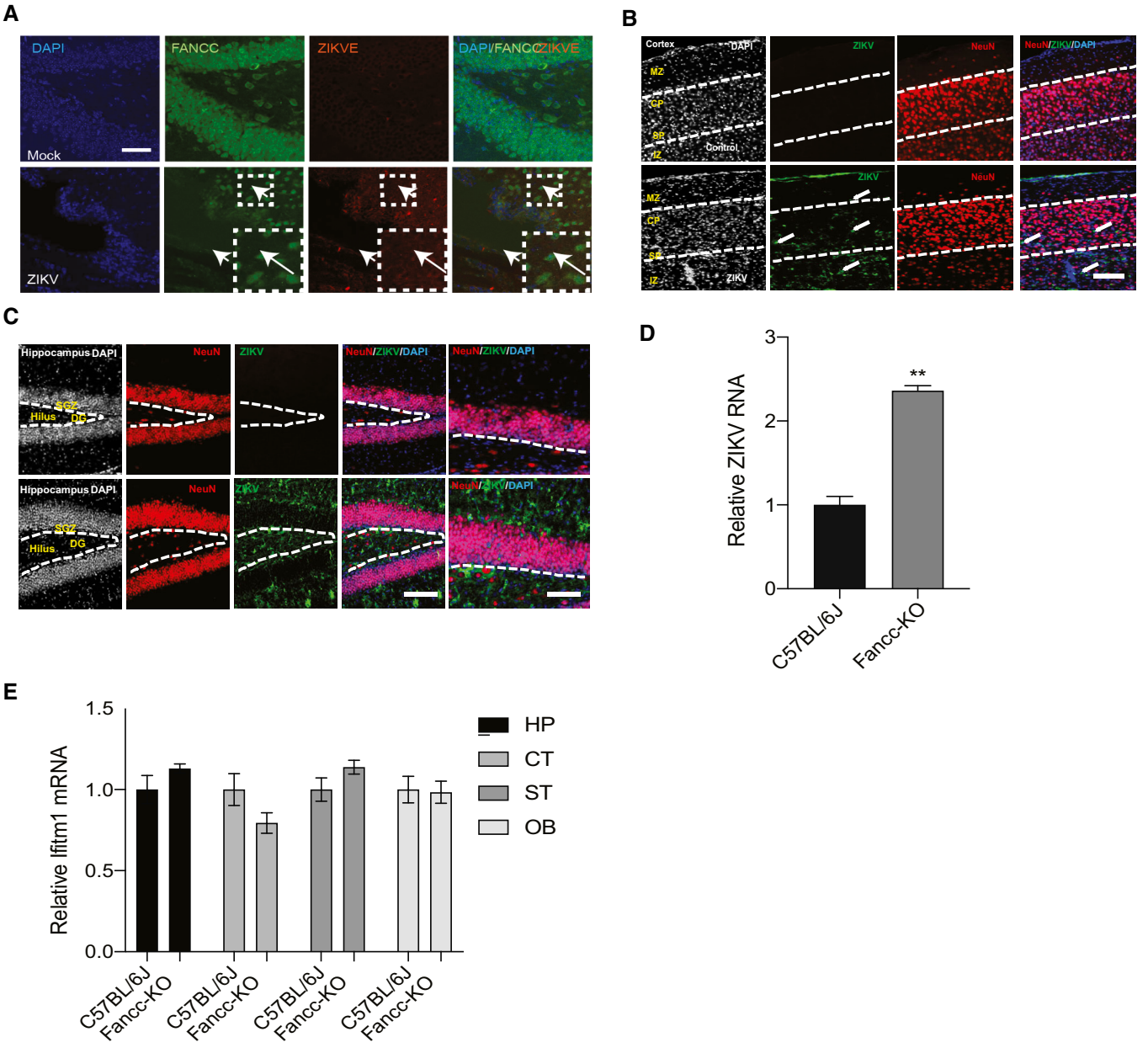


**Figure EV4. *In vivo* model of ZIKV infection.**

A Immunoreactivity of Fancc (green) with ZIKVE (red) in control and ZIKV-infected hippocampus brain region. Arrows represent reduction in Fancc immunoreactivity in ZIKV-infected cells, Scale bar = 50 μm.

B, C Immunostaining of mature neuronal marker NeuN (red) and ZIKV envelope flavivirus group antigen (ZIKVE, green) in the cortex (A), hippocampus (B) of uninfected or ZIKV Paraiba-infected *Ifnar*$^{-/-}$ mice 6 days post-infection. Nuclei were stained with DAPI (gray). DG, dentate gyrus; GCL, granular cell layer; InGr, internal granular layer; SGZ, subgranular zone. Scale bars are as indicated on image.

D RT-qPCR for ZIKV RNA expression in wild-type and *Fancc KO* mice brain infected with ZIKV. Mean ± SEM, $n$ = 3 biological replicates, $^{**}P < 0.001$ by Student's $t$ test.

E RT-qPCR for *Ifitm1* mRNA expression in wild type and *Fancc KO* mice brain. Mean ± SEM, $n$ = 3 biological replicates, ns by Student's $t$ test.